Synthesis and characterization of graphene oxide functionalized with magnetic nanoparticle via simple emulsion method

Synthesis and characterization of graphene oxide functionalized with magnetic nanoparticle via simple emulsion method

Emmellie Laura Albert[a,b], Che Azurahanim Che Abdullah[a,b,*], Yuki Shiroshaki[c]

[a] Materials Synthesis and Characterization Laboratory, Institute of Advance Technology, University Putra Malaysia, 43400 UPM Serdang, Selangor, Malaysia
[b] Department of Physics, Faculty of Science, University Putra Malaysia, 43400 UPM Serdang, Selangor, Malaysia
[c] Department of Materials Science, Faculty of Engineering, Kyushu Institute of Technology, 1-1 Sensui-cho, Tobata-ku, Kitakyushu-shi, Fukuoka 804-8550, Japan

ABSTRACT

Current research focusing on the loading of Iron (III) oxide (IO) onto graphene oxide (GO) via simple emulsion technique. GO specialty such as big surface to volume ratio combined with magnetic nanoparticle superparamagnetic properties produce interesting nanocomposite material for biomedical application. Proper modification was carried out by simply varying the ratios of GO to IO ranging from 1:1 to 1:3 to discover the best amount of IO suitable to be loaded on GO. In addition, the prepared nanocomposites crystallinity, chemical interaction, structure, surface morphology and magnetic behaviour were investigated using various equipment such as X-ray diffraction (XRD), Fourier transform infrared spectroscopy (FTIR), Raman spectroscopy (RAMAN), Vibrating Sample Magnetization (VSM), and Atomic force microscopy (AFM). The magnetic nanoparticle synthesized via co-precipitation method found to be Iron (iii) oxide. IO loaded with GO were validated to be superparamagnetic with maximum magnetic saturation measured at the ratio of GO to IO of 1:2.

Introduction

Magnetic nanoparticles (MNPs) has unique properties which enabled it to be guided and maintain at specific place by simply applying magnetic field. This outstanding property makes MNP suitable to be used in biomedical field. Iron (III) oxide (IO) was the most popular MNP used in biomedical field since it has the lowest toxicity [1]. MNPs had been repeatedly used in various field including biomedical field such as for application of magnetic cell sorting, hyperthermia, contrast agent in Magnetic Resonance Imaging (MRI) and immunoassay in pathology laboratories [2–5].

On the other hands, graphene oxide (GO) has garner significant attention due to its unique properties. It has honeycomb carbon geometry, two-dimensional (2D) crystal combined with one-atom thickness, large surface area, along with amazing electrical, optical, thermal, and mechanical properties. This amazing characteristic are originating from its chemical structures composed of sp^3 carbon domains adjoining sp^2 carbon domain and various functional groups such as hydroxyl, epoxy, and carboxyl groups [6]. Graphene comprises of a p-conjugated structure with six-atom rings on its sheet, which can be theoretically observed as a planar aromatic macromolecule [7]. This structure gives an outstanding ability to immobilize a large number of materials, including cells, drugs, biomolecules, metals, and fluorescent probes [8].

Hence, graphene has gain numerous interest especially in the nanomedicine and biomedical field [9]. For drug delivery application, GO offers great loading capacity and capability considering the loading ratio can go up to 200% which make it a suitable carrier for many biomolecules [10].

It is expected that the hybrids of IO and GO would have better functionalities and performances for these applications. GO with large specific surface area, makes the loading of IO onto GO possible [11]. The use of this hybrid as new framework material in cancer research can be very helpful both in locating the cancer and then curing the cancer by delivering the drug locally, thanks to the unique superparamagnetic properties of IO. For example, Szabo and coworkers (2008) successfully load tris(2,2′-bipyridl) Iron (II) ions on GO via ion exchange method followed by calcination process. Their prepared hybrid of magnetic graphene oxide showed a good electrical property [12]. In the following year, Yang et al. (2009) reported the preparation of GO–MNP hybrid through chemical precipitation technique and found that GO was loaded with 13.4 wt% of MNP. In addition they also successfully loaded the hybrid with an anti-cancer drug (doxorubicin hydrochloride). Owing to the superparamagnetic nature of the hybrid, it can be easily collected from water by applying an external magnetic field, hence showing the potential to be exploited in targeted drug delivery [13]. Recently, Cong and team revealed the possibility to

synthesize magnetic graphene by decorating MNP on the hydrazine-reduced GO sheets by means of high-temperature decomposition method and discover that the reduced GO attached to the MNP has the possibility to be used as magnetic resonance contrast agent [14].

To date, limited research had been conducted and focusing on the synthesis of hybrid nanoparticle made up of GO and decorated with MNP. Unlike the other work done by other researcher such as Yang et al. (2009) and Kyzas et al. (2013) this research focus on the optimization of MNPs to GO ratio [13,15]. In the biomedical application, the most important aspect of the nanohybrid made of magnetic graphene oxide is to attain the highest Ms so that it can be applied in the human body. In this project, we used different ratio of MNP to GO to investigate the nature of the hybrid as well as to get the optimized ratio of MNP to decorate GO.

Materials and method

Iron (II) chloride tetrahydrate ($FeCl_2 \cdot 4H_2O$, 99%), Iron (III) chloride hexahydrate ($FeCl_3 \cdot 6H_2O$, 99%), and Oleylamine ($C_{18}H_{37}N$, 70%) were purchased from Sigma-Aldrich. Ammonium hydroxide (NH_4, 32%) and chloroform ($CHCl_3$, 99%) were bought from R&M Chemicals. Nitrogen gas (N_2) was obtained from Air Product Malaysia. Graphene oxide was bought from GO advance solution, Malaysia.

Synthesis of Iron (III) oxide

IO were produced by the co-precipitation technique described previously by Mahdavi et al. [16]. Two types of iron, $FeCl_2 \cdot 4H_2O$ and $FeCl_3 \cdot 6H_2O$ were used. IO is prepared by simply mixing a base into an aqueous solution made up of Fe^{2+} (ferrous ion) and Fe^{3+} (ferric ion) chloride at a 1:2 M ratio. After that, the solution were dissolved in deionized water (DI) (150 mL). Next, 25 mL of NH_4 was mixed slowly to the previous mixture and stirred at 800 rpm and 45 °C. The precipitation produced was black in color. The production of IO must be conducted in an oxygen-free atmosphere because the reaction kinetics are affected by the oxidation speed of the iron species; therefore, N_2 gas was bubbles through the solution to avoid oxidation. Consequently, this will also decrease the size of the IO which is smaller in comparison to the method which did not remove oxygen as documented previously [17].

Synthesis of magnetic graphene oxide

Magnetic graphene oxide was synthesized by means of simple emulsion method. About 40 mg of GO were mixed with different amount of IO (40, 80, 120 mg). Initially, GO were mixed with chloroform (14 mL) and oleylamine (5 mL) through sonication process for about 1 h. Next, IO were sonicated in chloroform solution (5 mL) for 30 min. These two solutions were then mixed together by using probe sonicator for 30 min in an ice bath. After forming a homogenous solution, it was left overnight for drying purpose. The leftover solution was then washed using acetone. This process was repeated 3 times. Then, the final product was dried in an open air for 2 h and it was stored inside the dessicator. The final product was abbreviated as GO-IO.

Characterization of nanoparticle

GO (40 mg) loaded with different amount of IO (40, 80, 120 mg). The nanocomposite were abbreviated as GO-IO which were characterized by using various instruments such as X-ray diffraction (XRD) (Xpert pro, PANanalytical Philips, Netherland), Fourier Transform infrared spectroscopy (FTIR) (Nicolet 6700, Thermo Nicolet, USA), Transmission electron microscopy (TEM) (H-7650, Hitachi, Japan), RAMAN spectroscopy (RAMAN) (Alpha 300R, WITec, Germany), and Vibrating Sample Magnetometer (VSM) (Model 7404, Lake Shore, USA).
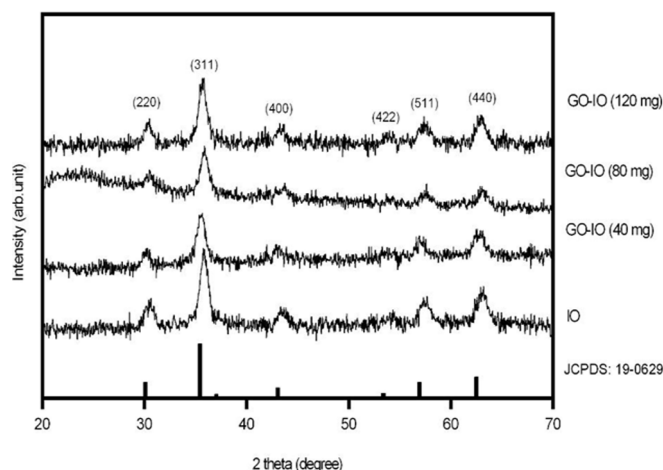

Fig. 1. XRD spectra of IO, GO-IO (40 mg), GO-IO (80 mg), and GO-IO (120 mg) including the JCPDS: 19-0629 for magnetite nanoparticle.
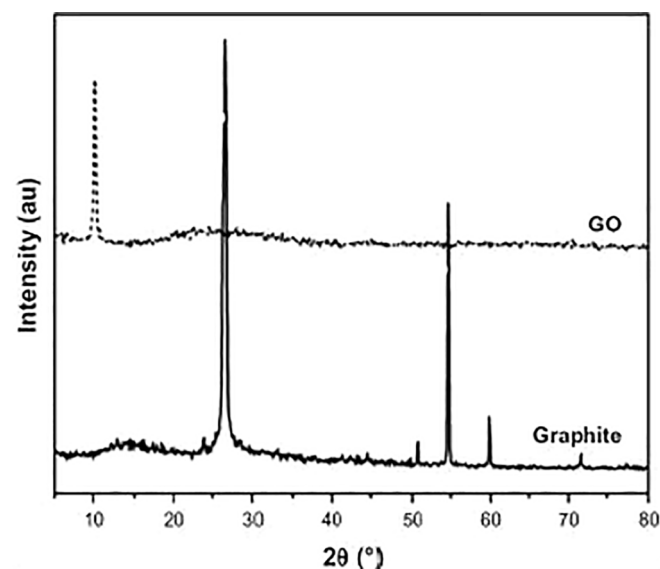

Fig. 2. XRD spectra of graphite and GO (sources: GO advance).

Discussion

X-ray diffraction

X-ray diffraction (XRD) pattern of the IO, GO, GO-IO (40 mg), GO-IO (80 mg), and GO-IO (120 mg) including the JCPDS: 19-0629 for magnetite are reveal in Fig. 1. All samples showed diffraction peaks at (2 2 0), (3 1 1), (4 0 0), (4 2 2), (5 1 1), and (4 4 0) of crystal planes belonging to Fe_3O_4 (JCPDS: 19–0629). Hence, indicating that the prepared composites contained magnetite. Graphite and GO XRD spectra showed diffraction peak assign to (0 0 2) plane for graphite and shift to (0 0 1) diffraction plane as presented in Fig. 2. Fig. 3 shows the XRD spectra of GO-IO (40 mg), GO-IO (80 mg), and GO-IO (120 mg) at 2 theta range from 5° to 15°, there are no peak belonging to GO detected due to the complete exfoliation of GO sheet and nanosolid of IO prevents the stacking of GO sheet as supported by previous work done by Zhang et al. [18] and Marcona [19].

Raman spectroscopy

Raman spectroscopy is a technique aimed at structural characterization of carbon-based materials. It offers information about the
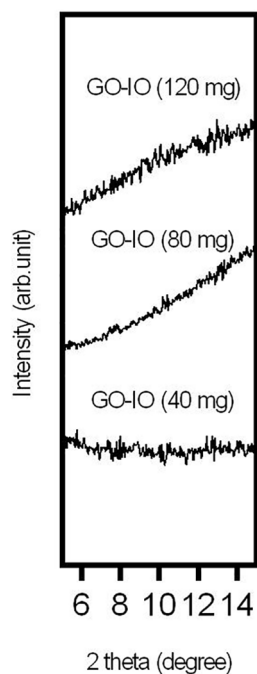
Fig. 3. XRD spectra of IO, GO-IO (40 mg), GO-IO (80 mg), and GO-IO (120 mg) at 2 theta degree ranging from 5° to 15°.
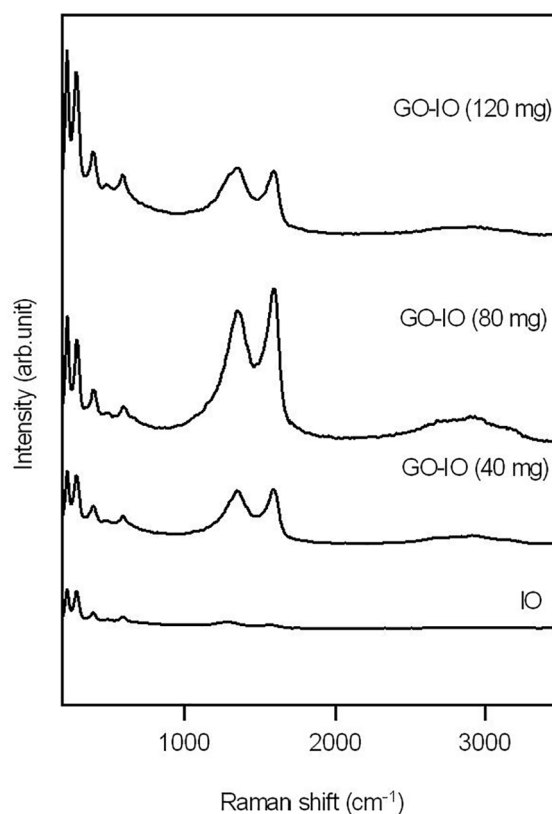

Fig. 4. Raman spectra of graphite and GO. ID/IG for GO is 0.94 (sources: GO advance).

Fig. 5. Raman spectra of IO, GO-IO (40 mg), GO-IO (80 mg), and GO-IO (120 mg).

Table 1
The ratio of I_D/I_G for GO-IO (40 mg), GO-IO (80 mg), and GO-IO (120 mg).

Samples	$R = I_D/I_G$
GO	0.94
GO-IO (40 mg)	1.02
GO-IO (80 mg)	0.93
GO-IO (120 mg)	0.99

structural changes during the chemical reactions for GO, GO-IO (40 mg), GO-IO (80 mg), and GO-IO (120 mg). Two obvious peaks were observed in Raman spectra shows in Figs. 4 and 5 displaying the D and G bands of GO. The D band indicated the vibrations of sp³ carbon atoms of disordered graphite whereas the G band associated to the E_2g mode of graphite, which refers to the in-plane vibration of sp² carbon atoms in a 2D hexagonal lattice [20,21]. The ratio of the peak intensity relative to the D to G band (ID/IG) is a valuable information used to assess the ordered and disordered crystal structures of carbon [22]. Table 1 listed the ratio of ID/IG for GO-IO (40 mg), GO-IO (80 mg), and GO-IO (120 mg).

For the GO-IO (40 mg), GO-IO (80 mg), and GO-IO (120 mg), the value of ID/IG ratio are 1.02, 0.93, and 0.99 respectively. The lowest value of ID/IG is for GO loaded with 80 mg of IO which is about 0.93 and increase to 0.99 as the amount of IO increased to 120 mg, while for GO loaded with only 40 mg of IO give the highest value of ID/IG ratio. This is due to the decreasing defect when GO is loaded with 80 mg of IO and increases when 40 mg of IO is loaded. In addition, the ID/IG for GO-IO (80 mg) is almost similar to the pure GO which is about 0.94.

Fourier transform infrared spectroscopy

The GO loaded with IO was further confirmed using FTIR. The FTIR spectra of GO, IO, GO-IO (40 mg), GO-IO (80 mg), and GO-IO (120 mg) are presented in Fig. 6. GO band at 1350 cm⁻¹ belong to the epoxy
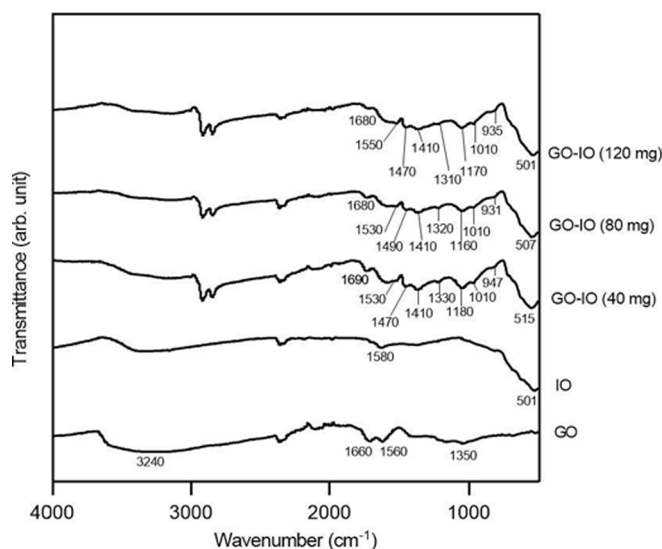
Fig. 6. FTIR bands for IO, GO, GO-IO (40 mg), GO-IO (80 mg), and GO-IO (120 mg).
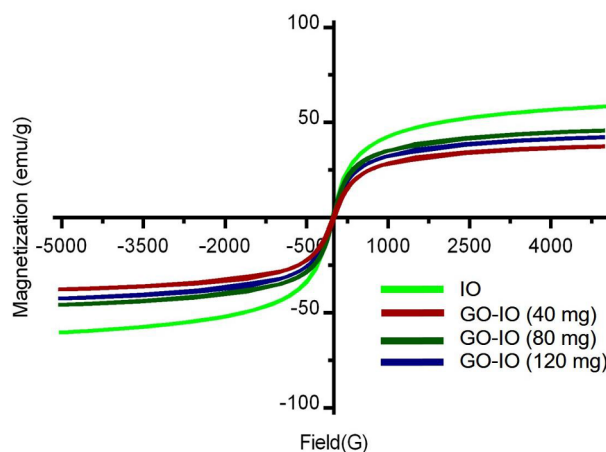

Fig. 7. VSM for IO, GO-IO (40 mg), GO-IO (80 mg), and GO-IO (120 mg). GO-IO (80 mg) has the highest Ms at 50 emu/g.

group; while 1560 cm^{-1} show the presence of aromatic rings; the band at 1660 is also for aromatic C=C can be assigned to the skeletal vibrations of unoxidized graphitic domains. In addition, O−H band can be observed in GO at 3240 cm^{-1}. The band observed at 501, 507, and 515 cm^{-1} are revealing the interaction occurred between Fe−O. The band observed at 2830, 2840 and 2890 cm^{-1} are assigned for asymmetric and symmetric C−H bonds respectively due to the interaction between GO and oleylamine [23]. The aromatic C=C stretching vibration is reveal at 1680, and 1690 cm^{-1} bands for the GO-IO nanocomposite. The C=C stretching band in aromatic ring at 1530, 1550, and 1580 cm^{-1} while the band at 1410, 1470, and 1490 cm^{-1} belong to the C−C bond in a ring. The C=C−H bond can be attributed by the band at 931, 935 and 945 cm^{-1}. This data is in agreement with the work done by Zhang et al. [24], Chaudhari et al. [25], and Wang et al. [26].

Vibrating sample magnetization

Magnetic hysteresis curves (Ms) obtained for IO, GO-IO (40 mg), GO-IO (80 mg), and GO-IO (120 mg) is shown in Fig. 7. There was no hysteresis curve observed for all samples which implying that all samples are superparamagnetic. The Ms value for IO, GO-IO (40 mg), GO-IO (80 mg), and GO-IO (120 mg) found to be 57.9, 40.7, 50.0, and 46.3 emu/g, individually. The highest Ms for the GO-IO nanocomposite is when the IO loaded is 80 mg because it has the highest content of IO as indicated in TGA results. The Ms of GO-IO (80 mg) is higher compared to several synthesize magnetic graphene oxide such as in the work done by Lei et al. (2014), Huang et al. (2015), and Han et al. (2012) with Ms of 40.2, 34.6, and 44.1 emu/g emu/g respectively [27–29]. The Ms is the highest for pure IO, the second highest is GO-IO (80 mg) followed by GO-IO (120 mg) while the lowest is GO-IO (40 mg). The IO content for GO-IO (80 mg) is the highest as indicated in TGA result hence it has the highest Ms. On the other hand, GO is a nonmagnetic material. So, the GO-IO (80 mg) which has the highest Ms is the best for biomedical field since it will enable the nanocomposites to be retain at a specific site of the body.

Thermalgravimetric analysis

The TGA curves of GO-IO present a characteristic peak from 225 to 553 °C. Table 2 is the summaries of the weight loss according to temperature. All of the composites showed 2 step weight loss. The first weight loss is due to the evaporation of the moisture followed by the removal of O−H group attached to the GO in relation to the first and second DTG peak which was supported by the work done by Zhang et al. [24]. The second weight loss is the degradation of GO

Table 2
The weight loss of GO-IO (40, 80, 120 mg) according to step of weight loss.

Step	Weight loss (%)		
	GO-IO (40 mg)	GO-IO (80 mg)	GO-IO (120 mg)
1	14	20	23
2	34	23	23
Residue	52	57	54

corresponding to the DTG third peak. Previous research done by Mahdavi et al. (2013), found that phase transition of Fe_3O_4 to FeO occurred at temperature above 500 °C therefore the residue is indicating the presence of IO [16]. From the table, GO-IO (80 mg) has the highest amount of IO followed by the GO-IO (120 mg) and GO-IO (40 mg) which is about 57, 54, and 52% respectively. GO has reach the point of saturation for loading IO therefore it no longer able to load IO (Fig. 8).

Atomic force microscopy

The morphology of the GO and the GO-IO nanocomposites were examined by means of AFM. The profile for single layer GO which indicated that the single sheet GO possess a height of about 1 nm is displayed in the Fig. 9. After IO of different amount was loaded on to the GO, many spherical surface bumps are detected on the surface of the GO-IO nanocomposite, which represent IO which also include its height profile (Fig. 10). GO-IO (80 mg) has the lowest height profile compared to the other GO-IO nanocomposites which revealed that GO-IO (80 mg) have the smallest size. The nanocomposites with the highest height profile means that the IO in the GO-IO (40 mg) has a bigger size compared to the other samples.

Tranmission electron microscopy

TEM was used to observe the morphologies of GO-IO (40, 80, and 120 mg). As shown in Fig. 11, the small spherical nanoparticles is IO. IO tend to aggregate due to its small size. GO is observed as an irregular shape sheet with wrinkled. Fig. 11 shown that the IO were decorated on GO. The IO are disorderly distributed on the GO sheet. In the images
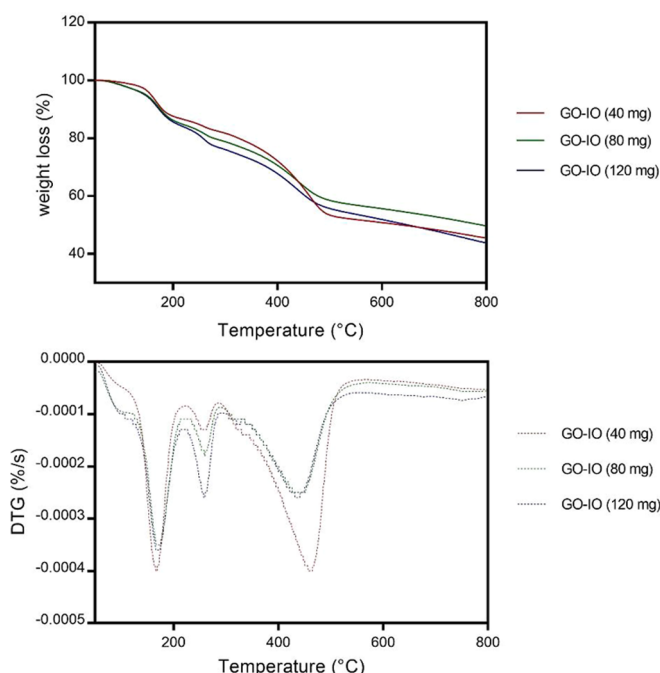

Fig. 8. TGA and DTG curve showed three step weight loss at temperature range 50 °C to 800 °C for GO-IO (40 mg), GO-IO (80 mg), and GO-IO (120 mg).
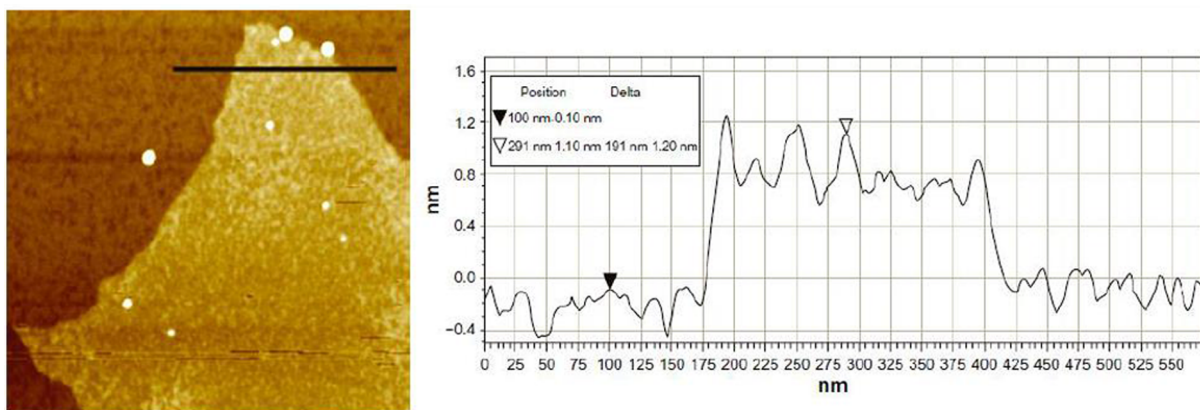

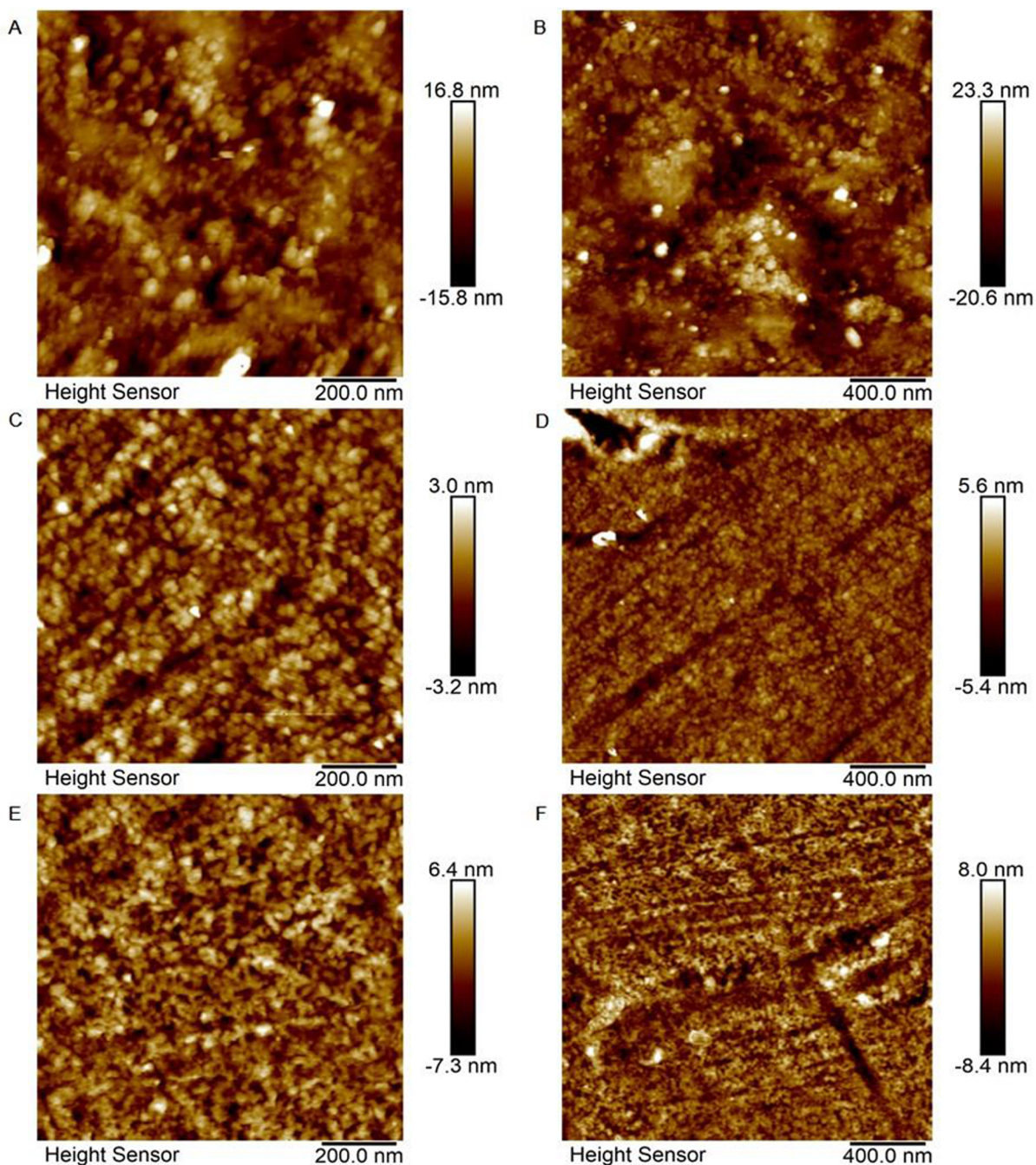**Fig. 9.** AFM profile of single layer Graphene Oxide (sources: GO advance).

Fig. 10. AFM images profile for (A) GO-IO (40 mg) (C) GO-IO (80 mg) and (E) GO-IO (120 mg) at higher magnification while (B) GO-IO (40 mg) (D) GO-IO (80 mg) and (F) GO-IO (120 mg) at lower magnification.
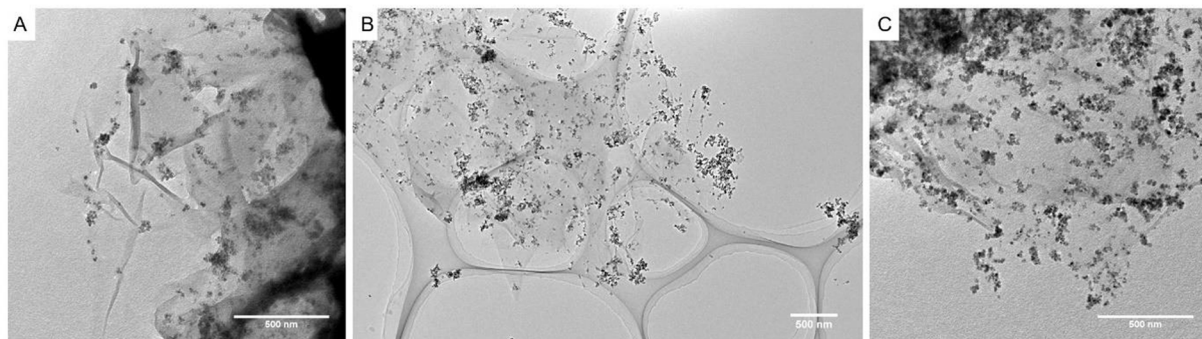

Fig. 11. TEM images of A) GO-IO (40 mg), B) GO-IO (80 mg), and GO-IO (120 mg) showing the IO were decorated on GO.

taken, some IO were not anchored to the GO this might be due to the sonication process during the sample preparation. The sonication step is a must in the sample preparation for TEM.

Conclusion

This study revealed the loading of GO with different amount of IO (40, 80, and 120 mg). The IO were successfully conjugated on GO using simple emulsion method. XRD data confirmed that after loading of IO on GO, the GO main peak disappears indicating that the GO stacking is prevented by the present of IO. In addition, the size of the IO loaded to GO found to be the smallest size when IO loaded is 80 mg. In addition, the Ms of the optimized GO-IO is 50 emu/g, which is favourable for further used in the biomedical field such as targeted drug delivery application since it enables the nanocomposites to be retained at the specified and selected areas of the body. In the future, we believe that our synthesized nanocomposites have high potential to be applied in the biomedical field specifically for the targeted drug delivery system.

Acknowledgments

Conflicts of interest

The authors declare no conflict of interest.

Appendix A. Supplementary data

Supplementary data to this article can be found online at https://doi.org/10.1016/j.rinp.2018.10.054.

References

[1] Kolesnichenko, V., et al., Iron oxide nanoparticles with a variable size and an iron oxidation state for imaging applications; 2016.

[2] Pamme N, Wilhelm C. Continuous sorting of magnetic cells via on-chip free-flow magnetophoresis. Lab Chip 2006;6(8):974–80.

[3] Johannsen M, et al. Magnetic nanoparticle hyperthermia for prostate cancer. Int J Hyperth 2010;26(8):790–5.

[4] Kim EH, et al. Synthesis of ferrofluid with magnetic nanoparticles by sonochemical method for MRI contrast agent. J Magn Magn Mater 2005;289:328–30.

[5] Nikitin PI, Vetoshko PM, Ksenevich TI. New type of biosensor based on magnetic nanoparticle detection. J Magn Magn Mater 2007;311(1):445–9.

[6] Rostamizadeh S, Hemmasi A, Zekri N. Magnetic amine-functionalized graphene oxide as a novel and recyclable bifunctional nanocatalyst for solvent-free synthesis of pyrano[3,2-c]pyridine derivatives. Nanochem Res 2017;2(1):29–41.

[7] Chen D, Feng H, Li J. Graphene oxide: preparation, functionalization, and electrochemical applications. Chem Rev 2012;112(11):6027–53.

[8] Liu J, Cui L, Losic D. Graphene and graphene oxide as new nanocarriers for drug delivery applications. Acta Biomater 2013;9(12):9243–57.

[9] Gurunathan S, Kim J-H. Synthesis, toxicity, biocompatibility, and biomedical applications of graphene and graphene-related materials. Int J Nanomed 2016;11:1927–45.

[10] Yin PT, et al. Design, synthesis, and characterization of graphene–nanoparticle hybrid materials for bioapplications. Chem Rev 2015;115(7):2483–531.

[11] Urbas K, et al. Chemical and magnetic functionalization of graphene oxide as a route to enhance its biocompatibility. Nanoscale Res Lett 2014;9(1):656.

[12] Szabó T, et al. Magnetically modified single and turbostratic stacked graphenes from tris(2,2′-bipyridyl) iron(ii) ion-exchanged graphite oxide. J Phys Chem B 2008;112(46):14461–9.

[13] Yang X, et al. Superparamagnetic graphene oxide–Fe_3O_4 nanoparticles hybrid for controlled targeted drug carriers. J Mater Chem 2009;19(18):2710–4.

[14] Cong HP, et al. Water – soluble magnetic-functionalized reduced graphene oxide sheets: in situ synthesis and magnetic resonance imaging applications. Small 2010;6.

[15] Kyzas GZ, et al. Magnetic graphene oxide: effect of preparation route on reactive black 5 adsorption. Materials 2013;6(4):1360–76.

[16] Mahdavi M, et al. Synthesis, surface modification and characterisation of biocompatible magnetic iron oxide nanoparticles for biomedical applications. Molecules 2013;18(7):7533–48.

[17] Ali A, et al. Synthesis, characterization, applications, and challenges of iron oxide nanoparticles. Nanotechnol Sci Appl 2016.

[18] Zhang M, Jia M, Jin Y. Fe_3O_4/reduced graphene oxide nanocomposite as high performance anode for lithium ion batteries. Appl Surface Sci 2012;261(Supplement C):298–305.

[19] Marcano DC, et al. Improved synthesis of graphene oxide. ACS Nano 2010;4(8):4806–14.

[20] Zhang W, et al. A strategy for producing pure single-layer graphene sheets based on a confined self-assembly approach. Angew Chem Int Ed 2009;48(32):5864–8.

[21] Wu J-B, et al. Raman spectroscopy of graphene-based materials and its applications in related devices. Chem Soc Rev 2018;47(5):1822–73.

[22] Araujo PT, Terrones M, Dresselhaus MS. Defects and impurities in graphene-like materials. Mater Today 2012;15(3):98–109.

[23] Sasikala ARK, et al. Multifunctional nanocarpets for cancer theranostics: remotely controlled graphene nanoheaters for thermo-chemosensitisation and magnetic resonance imaging. Sci Rep 2016;6:20543.

[24] Zhang J, et al. Poly (acrylic acid) functionalized magnetic graphene oxide nanocomposite for removal of methylene blue. RSC Adv 2015;5(41):32272–82.

[25] Chaudhari NS, et al. Graphene oxide based magnetic nanocomposites for efficient treatment of breast cancer. Mater Sci Eng, C 2014;37:278–85.

[26] Wang G, et al. Multifunctional Fe_3O_4/graphene oxide nanocomposites for magnetic resonance imaging and drug delivery. Mater Chem Phys 2013;141(2–3):997–1004.

[27] Lei Y, et al. Three-dimensional magnetic graphene oxide foam/Fe_3O_4 nanocomposite as an efficient absorbent for Cr (VI) removal. J Mater Sci 2014;49(12):4236–45.

[28] Huang Y, et al. Magnetic graphene oxide modified with choline chloride-based deep eutectic solvent for the solid-phase extraction of protein. Anal Chim Acta 2015;877:90–9.

[29] Han Q, et al. Facile and tunable fabrication of Fe3O4 graphene oxide nanocomposites and their application in the magnetic solid-phase extraction of polycyclic aromatic hydrocarbons from environmental water samples. Talanta 2012;101:388–95.